JACS
JOURNAL OF THE AMERICAN CHEMICAL SOCIETY
pubs.acs.org/JACS
Article

Characterizing Chelation at Surfaces by Charge Tunneling

Yuan Li,[⊥] Samuel E. Root,[⊥] Lee Belding, Junwoo Park, Jeff Rawson, Hyo Jae Yoon, Mostafa Baghbanzadeh, Philipp Rothemund, and George M. Whitesides*

Cite This: J. Am. Chem. Soc. 2021, 143, 5967−5977
Read Online
ACCESS | Metrics & More | Article Recommendations | Supporting Information

ABSTRACT: This paper describes a surface analysis technique that uses the "EGaIn junction" to measure tunneling current densities (J(V), amps/cm^2) through self-assembled monolayers (SAMs) terminated in a chelating group and incorporating different transition metal ions. Comparisons of J(V) measurements between bare chelating groups and chelates are used to characterize the composition of the SAM and infer the dissociation constant (K_d, mol/L), as well as kinetic rate constants (k_{off}, L/mol·s; k_{on}, 1/s) of the reversible chelate-metal reaction. To demonstrate the concept, SAMs of 11-(4-methyl-2,2′-bipyrid-4′-yl (bpy))undecanethiol ($HS(CH_2)_{11}$bpy) were incubated within ethanol solutions of metal salts. After rinsing and drying the surface, measurements of current as a function of incubation time and concentration in solution are used to infer k_{off}, k_{on}, and K_d. X-ray photoelectron spectroscopy (XPS) provides an independent measure of surface composition to confirm inferences from J(V) measurements. Our experiments establish that (i) bound metal ions are stable to the rinsing step as long as the rinsing time, $\tau_{rinse} \ll \frac{1}{k_{off}}$; (ii) the bound metal ions increase the current density at the negative bias and reduce the rectification observed with free bpy terminal groups; (iii) the current density as a function of the concentration of metal ions in solution follows a sigmoidal curve; and (iv) the values of K_d measured using J(V) are comparable to those measured using XPS, but larger than those measured in solution. The EGaIn junction, thus, provides a new tool for the analysis of the composition of the surfaces that undergo reversible chemical reactions with species in solution.

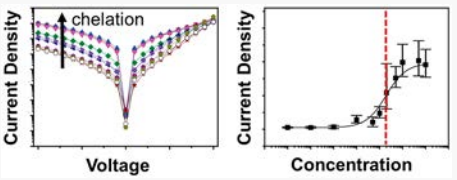

INTRODUCTION

The fundamental mechanisms of charge transport by tunneling through organic matter that is insulating to electron drift conduction[1] remain incompletely understood. They are, however, relevant to a range of subjects including redox biochemistry, catalysis, as well as organic and molecular electronics. Charge tunneling through covalently bound organic compounds has been studied extensively, but comparable investigations of charge tunneling through transition metal coordination complexes are few.[2,3] The ability to measure charge tunneling through coordination complexes has the potential to broaden the range of tunneling processes that can be conveniently examined, and open new classes of molecules whose transport properties can be understood. Moreover, measured changes in charge tunneling due to the formation of coordination complexes can be used as a simple way to characterize the composition of the surface, and thus have the potential to serve as an analytical tool to study interactions at surfaces.

Complexes of transition metals with organic compounds range in their stabilities from high (e.g., ferrocene and many complexes of ethylenediaminetetraacetic acid with metal ions) to weak. Charge tunneling through weakly bound complexes has been difficult to study using ex situ methods because molecular assemblies that are not covalently bound can dissociate during the preparation or handling of samples. We report here an analytical procedure that uses electrical measurements of charge tunneling to characterize the binding of metal ions to 2,2′-bipyridine (bpy) ligands that are built into self-assembled monolayers (SAMs). The procedure uses a eutectic gallium−indium (EGaIn) junction, with a contact area between the electrode and the SAM of ∼1000 μm^2, to measure changes in tunneling current density (J(V), amps/cm^2) through an ensemble of molecules, and monitor the progression from a SAM of uncomplexed ligands to one saturated with metal ions. Our titration procedure involves the following steps (Figure 1): (i) incubate SAMs in contact with solutions that contain various concentrations of transition metal ions; (ii) remove SAMs from the solutions and rinse; (iii) dry SAMs under a stream of nitrogen; and (iv) measure the tunneling current, J(V), across the SAMs with the EGaIn electrode.

In this paper, we demonstrate that the binding of metal ions to SAMs terminated by bpy groups changes the tunneling current density across them, and that this change can be used to infer the composition of the SAM. We use the measurements of tunneling currents to determine the rates of

Received: February 15, 2021
Published: April 9, 2021

https://doi.org/10.1021/jacs.1c01800
J. Am. Chem. Soc. 2021, 143, 5967−5977

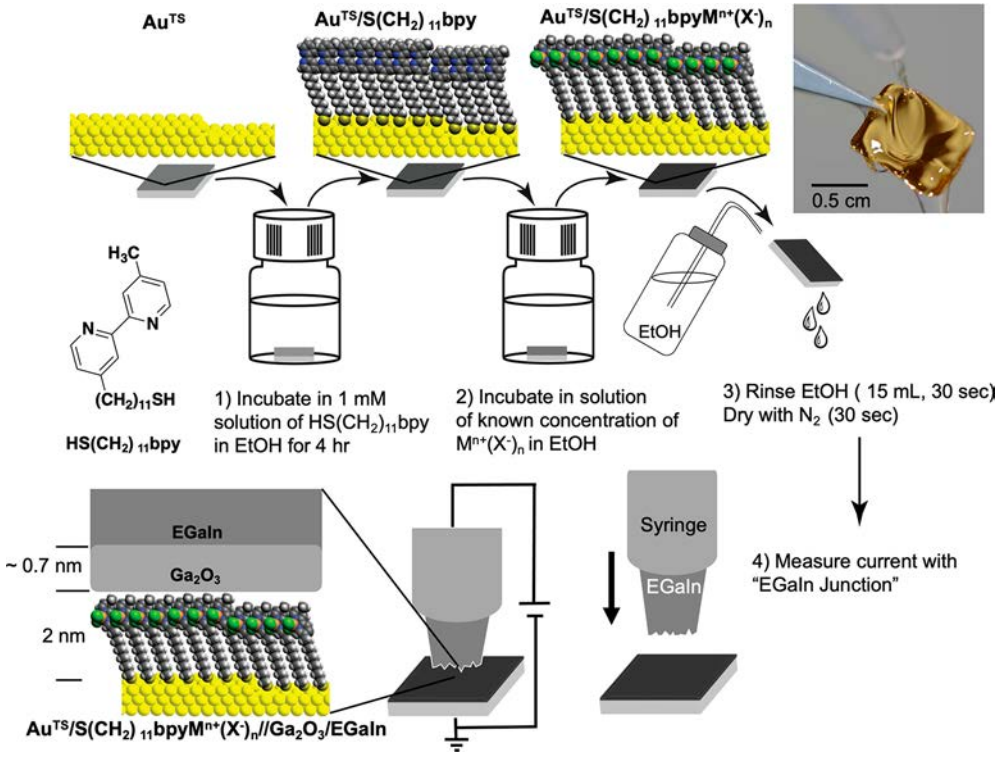

Figure 1. Schematic diagram illustrating the workflow for a tunneling titration experiment for junctions of the form $Au^{TS}/S(CH_2)_{11}bpyM^{n+}(X^-)_n//Ga_2O_3/EGaIn$. The inset photograph shows the rinsing process. The roughness and shape of the tip is indicated only schematically and is not to scale, and the monolayer may not be as ordered as indicated.

association and dissociation for several metal ions with these SAMs, and the equilibrium dissociation constants of the binding reactions, and also to evaluate the competitive binding of two ions. We validate the charge tunneling measurements, which are conceptually and experimentally simple, with X-ray photoelectron spectroscopy (XPS).

We expect this technique will be useful in studying equilibrium binding and charge transport through a variety of supramolecular complexes on surfaces. By working with SAMs—which are uniquely well-defined organic surfaces—this method is amenable to any chemical group that can be bonded to an electrode, with implications for catalysis, bioinorganic chemistry, and sensing.

BACKGROUND

Characterization of Non-Covalent Binding at Surfaces. The noncovalent interactions of chemical species on surfaces are, in general, different than those in solution. The thermodynamic equilibrium between the associated and dissociated states may differ because of differences in solvation. Conformational restrictions associated with a densely packed surface prevent many binding geometries and may change the stoichiometry of binding that is energetically preferred. Noncovalent binding between chemical species in bulk solution and receptors on the surface of SAMs has been examined previously with a variety of surface sensitive techniques, including surface plasmon resonance spectroscopy,[4] quartz crystal microgravimetry,[5] and electrochemical methods.[6,7] Additionally, measured changes in the electrical conductance of single-molecule junctions as a function of pH have previously been employed to titrate individual molecules.[8]

Charge Tunneling across Transition Metal Complexes. The "EGaIn Junction" uses a eutectic gallium−indium top electrode covered with a self-limiting thin film of gallium oxide (Ga_2O_3, ostensibly ∼0.7 nm thick, but thicker in portions of the junctions where it has buckled).[9,10] Transport measurements through the EGaIn junction sample ensembles of the molecules within a contact area of ∼1000 μm^2, and are dominated by charge tunneling through the molecules, rather than by the Ga_2O_3 layer.[11−13] The great majority of studies by our group,[11−14] Nijhuis,[15−17] Chiechi,[18,19] Yoon,[20−23] and others[24,25] on charge tunneling through SAMs with the EGaIn junction have employed the methods of physical organic chemistry, where measurements as a function of regularly varied molecular structure are compared to infer mechanistic details and chemical design rules.[26]

Fewer studies, however, have investigated charge transport through molecules where variations were mediated by coordination chemistry.[15,27] In one example, Vuillaume and co-workers demonstrated that the binding of a Pb^{2+} cation to a SAM presenting a crown ether loop-derivatized oligothiophene produced a large increase in current density, induced by a shifting of the frontier molecular orbitals toward the Fermi levels of the electrodes.[28] In another example, You, Therian, and co-workers showed that charge tunneling properties of SAMs of conjugated porphyrin oligomers are influenced by differences in the chelated metal ions, due to differences in the energy levels of the frontier molecular orbitals of the complexes.[29] In a final example, Rampi and co-workers grew conductive molecular wires (∼ 40 nm long) on a gold surface via sequential stepwise coordination of metal ions by terpyridine-based ligands; the conductivity of these molecular wires were also found to depend upon the proximity of the frontier molecular orbitals of the complexes to the Fermi levels of the electrodes.[30] None of these studies, however, have used the measured changes in current densities as an analytical tool

https://doi.org/10.1021/jacs.1c01800
J. Am. Chem. Soc. 2021, 143, 5967−5977

Table 1. Summary of Metal−Chelate Dissociation Constants in Solution and on the Surface of SAMs

metal ion	phase	chelate	counter ion	solvent[a](prepare→ measure)	titration method	K_d (mol/L)	ref.[b]
Cu^{2+}	solution	bpy	Cl^-	water	UV−vis	7×10^{-9}	30
	solution	bpy	$(NO_3)^-$	ethanol/water 1:1	potentiometry	8.7×10^{-9}	33
	surface	bpy	Cl^-	ethanol→air	EGaIn	1.9×10^{-5}	†
	surface	bpy	Cl^-	ethanol→vacuum	XPS	4.7×10^{-6}	†
Ni^{2+}	solution	bpy	Cl^-	water	UV−vis	8.5×10^{-8}	30
	surface	bpy	Cl^-	ethanol→air	EGaIn	1.3×10^{-4}	†
	surface	bpy	Cl^-	ethanol→ vacuum	XPS	9.4×10^{-5}	†
Ag^+	solution	bpy	$(NO_3)^-$	ethanol/water 1:1	potentiometry	1.9×10^{-4}	33
	surface	bpy	ClO_4^-	ethanol→air	tunneling	7.6×10^{-6}	†
	surface	bpy	ClO_4^-	ethanol→vacuum	XPS	3.3×10^{-6}	†

[a]"/" indicates a mixture and "→" indicates the sequence of incubation and drying of the surface in our method of measurement. [b]"†" indicates this work.

to characterize the chemical kinetics or thermodynamics of the reversible binding reaction.

Rectification in bpy-Terminated SAMs. We chose bpy as the chelating group for several reasons: (i) bpy is a prototypical ligand in coordination and supramolecular chemistry;[31] (ii) 11-(4-methyl-2,2′-bipyrid-4′-yl (bpy))-undecanethiol ($HS(CH_2)_{11}$bpy) has been shown to form tightly packed, well-ordered SAMs terminated with bpy groups;[20,21,32] and (iii) stable complexes of bpy with many transition metal cations form spontaneously at room temperature.[33,34]

Previous work by our group has demonstrated that SAMs terminated in bpy groups rectify tunneling current with a rectification ratio, $R = |J(+1.0\ V)|/|J(-1.0\ V)| = 85 \pm 2$, when incorporated into junctions of the form $Ag^{TS}/S(CH_2)_{11}$bpy//Ga_2O_3/EGaIn.[32] That is, in these junctions, at an applied bias of +1.0 V (when EGaIn is oxidizing relative to Ag), the rate of charge tunneling is faster than that at −1.0 V (when EGaIn is reducing relative to Ag). This rectification is due to the bpy unit, and not the redox behavior of Ga_2O_3, Ga, In, or Ag^{TS} (or Au^{TS}) components of the tunneling junction; the possibility of bpy chelation to metals from the EGaIn electrode was also eliminated.[32] Rectification in bpy-terminated SAMs occurs by a mechanism analogous (but of opposite polarity) to that which occurs in the more extensively studied ferrocene-based system.[16,17,35] At positive bias the LUMO on the bpy unit mediates charge transport, resulting in a reduction in the effective tunneling barrier width in comparison to a negative bias. Moreover, we have recently demonstrated that the binding of transition metal ions to the bpy unit can alter the energy levels of the frontier molecular orbitals and produce changes in current density that are dependent upon the identity of the metal ion.[36]

Characterization of Transition Metal Complexes in Solution. In solution, a range of metal cations (Cu^{2+}, Ni^{2+}, Zn^{2+}, Ag^{1+}) form complexes with 2,2′-bipyridine (bpy) spontaneously at room temperature. These complexes can involve the coordination of one, two, or three bpy groups ($[M^{n+}(bpy)X_n^-]$, $[M^{n+}(bpy)_2X_n^-]$, and $[M^{n+}(bpy)_3X_n^-]$ (M = transition metal, X^- = counteranion), with distinct association constants K_1, K_2, and K_3.[33,34] The measurement of these association constants was not trivial because species of different coordination number are simultaneously present, but it was accomplished using careful experimental design and standard analytical techniques.

Irving and Mellor definitively characterized the equilibria of association for bpy with the bivalent cations of the first-row transition metals. These authors employed a biphasic titration method with spectrophotometric analysis to measure the equilibria of formation for the 1:1, 1:2, and 1:3 complexes of metal/bpy. Values for the K_d of the 1:1 complexes of bpy with Cu^{2+} and Ni^{2+} determined from these results are given in Table 1.[33] Scrocco and co-workers characterized the equilibria of association for Cu^{2+} with bpy in solutions of water and ethanol, with $(NO_3)^-$ as the counterion (see Table 1 for details).[37] Importantly, values of K_d determined from these measurements depend weakly (remain within the same order of magnitude) on the ratio of ethanol to water, and agree well with those determined by Irving and Mellor for chlorides in water. This agreement indicates that the value of K_d is relatively unaffected by the solvent (ethanol vs water), or the counterion ($(NO_3)^-$ vs Cl^-), although this may not be true in general for different solvents and counterions. The Irving-Williams order is a stability series for complexes of first-row bivalent metals that is upheld across many classes of ligands: Mn < Fe < Zn < Co < Ni < Cu.[34] The stabilities of the 1:1 complexes of these ions with bpy in solution follow this order.[33]

EXPERIMENTAL SECTION

Preparation of the SAMs of bpy−M^{n+}. We prepared the SAMs of $Au^{TS}/S(CH_2)_{11}$bpy as reported previously, by immersing Au^{TS} substrates (~1 cm^2) in ethanolic solutions containing ~1 mM $HS(CH_2)_{11}$bpy.[32] We used gold rather than silver substrates because they are more resistant to oxidation, allowing us to perform experiments with long incubation times without concern for the quality of our inert atmosphere. Unlike for other rectifiers,[35] the high rectification ratio of $HS(CH_2)_{11}$bpy is reliably retained on Au^{TS}.[32,38,39]

We examined the binding equilibria of bpy-terminated SAMs in ethanol solutions of three different metal salts: $CuCl_2$, $NiCl_2$, and $AgClO_4$ (because AgCl is insoluble in ethanol and water). Anhydrous ethanol was used instead of water to minimize the potential oxidation of the SAM during the time period of incubation with the metal salt. An initial screening of metal salts showed that treatment of bpy-terminated SAMs Cu^{2+}, Ni^+, and Ag^+ all produced $J-V$ curves that differed significantly from those of untreated SAMs. To prepare the metalated samples, we immersed the ~1 cm^2 chip supporting the SAMs (glass/OA/$Au^{TS}/S(CH_2)_{11}$bpy, where OA is Norland 61 optical adhesive) in solutions of varied concentrations, ranging from 10^{-9} to 10^{-3} mol/L under N_2 at room temperature. The solutions of metal salts with concentrations below 10^{-6} mol/L were prepared by serial dilution from stock solutions of 10^{-6} mol/L to reach concentrations from 10^{-7} to 10^{-9} mol/L. The serial dilutions were performed by transferring (using a 10 mL glass Hamilton syringe) 50 mL of the respective stock solution to a 500 mL analytical volumetric flask, which was then carefully filled to the mark with anhydrous ethanol (purchased from Sigma-Aldrich in anhydrous form).

https://doi.org/10.1021/jacs.1c01800
J. Am. Chem. Soc. 2021, 143, 5967−5977

Volumes of the solutions for incubation of SAMs ranged from 3 mL to 5 L, depending on the concentration, to ensure at least ×100 excess of metal ions in solution compared to bpy sites (~8×10^{-9} mol/cm^2, as measured by XPS) on the surface. After at least 3 h, or at most 12 h of immersion (lower concentrations were incubated longer), we used plastic forceps (to avoid metal contamination) to pick up the samples, gently rinsed them for 30 s with ~15 mL of EtOH to remove physically adsorbed metal salts (Figure 1) and dried them under a gentle stream of house N_2 (evaporated from liquid N_2). The rinsing and drying procedure was used for all measurements reported in this work. We observed excess metal ions (~5% to 15% determined by XPS) in SAMs that were measured without rinsing after removal from solutions containing 10^{-3} mol/L of salt.

Current Density Measurements. We measured the tunneling current through the SAMs of $Au^{TS}/S(CH_2)_{11}bpy$ and $Au^{TS}/S(CH_2)_{11}bpy(M^{n+})X_n^-$ from 0 V to ±1.0 V, at 0.1 V intervals, and analyzed the J–V (current density, J (A/cm^2), as a function of applied voltage V) traces for each SAM (~500 curves). We followed a standard "1/20/1" protocol[13] for the collection of J(V) data; that is, we used each tip only for a single contact. For each junction, the EGaIn tip was brought into contact with the SAM once with a contact area of ~1000 μm^2 and a contact pressure of ~2.5 kPa,[40] and the voltage range (−1.0 to 1.0 V) was scanned 20 times.

To form an EGaIn tip, we extruded a drop of EGaIn from a 10-μL Hamilton syringe held by micromanipulator and brought the drop into contact with a bare Au surface. We used the micromanipulator to pull up the drop of EGaIn and draw it into an hourglass shape until it broke at the thinnest region of the neck, forming a tip.[40] That tip was used to form a junction used for 20 J–V scans, and then discarded, and we formed a new tip on a bare Au surface for the next junction.

Statistical Analysis. We formed junctions containing each type of SAM on three different chips and formed 7 to 9 junctions on each chip. Thus, for each type of SAM we recorded the J–V characteristics of 21 to 27 junctions, and thus obtained a total of 504 to 648 J(V) traces. The procedure used for the statistical analysis of the data has been reported before,[13,41] but we give a brief description here.

We treat the values of J and R as log-normally distributed (although in practice we know they often are not; see the Supporting Information, SI, S2 for histograms of the data). We defined the values of $R = J(+1.0\ \text{V})/J(-1.0\ \text{V})$. We calculated the mean values ($\langle J\rangle$; $\langle R\rangle$) and one standard deviations (σ) of J and R from the Gaussian fits to the histogram of $|J|$ and $|R|$ plotted on a scale of log(J) or log(R). We calculated the 95% confidence intervals (CI) using Z-test: $\text{CI} = z_{\alpha/2}\sigma/\sqrt{N}$ where $z_{\alpha/2}$ is the inverse of the cumulative distribution function for the standard normal distribution.[41] For the 95% confidence interval ($\alpha = 0.05$), $z_{\alpha/2}$ is equal to 1.96. The value of N is the number of independently measured current densities, from distinct junctions (21–27). That is, since values of J measured using the same junction are probably correlated, we consider N as the number of junctions, not the total number of J–V traces.[41]

X-ray Photoelectron Spectroscopy (XPS). We employed XPS to measure: (i) the oxidation states of the metal cations in the SAMs, through comparison to known standards of binding energies (Thermo Scientific, Avantage XPS database). (ii) The stoichiometry/composition of the complexes—the elemental ratio was calculated by dividing the integrated area of the Cu $2p_{3/2}$, Ni $2p_{3/2}$, or Ag $3d_{5/2}$ peaks by the integrated area of the N 1s peak (after normalizing for differences in photoionization cross sections among atoms). We expect percentage atomic compositions derived from XPS to be accurate since the nitrogen, metal atoms, and counterions, are located at the top of the monolayer, and effects due to attenuation of photoelectrons from those atoms are negligible.[42] (iii) The stoichiometry of the anions, by comparing the elemental ratio of Cl to the metal cations. Short acquisition times of ~300 s for each XPS spectrum were used to minimize damage to the sample and reduction of metal ions by photoelectrons.

RESULTS AND DISCUSSION

Equilibrium Binding Model. We modified the classical Langmuir adsorption model[43] to determine the free energy of binding of the metal cations to the bpy-terminated SAMs. This model uses the following assumptions: (i) a 1:1 binding stoichiometry between bpy and metal (this assumption was justified by XPS measurements and the quality of the fit of the experimental data to the model); (ii) we assume the concentration of metal ion in solution, [M] (mol/L), is constant due to a large molar excess of metal ions in solution compared to surface sites. Our experiments were specifically designed such that the number of molecules on the surface (~8×10^{-9} mol for a typical sample with a surface of 1 cm^2) were insignificant relative to the number in of metal ions solution (e.g., 1 mM solution of $CuCl_2$ in 3 mL of ethanol contains 3×10^{-6} mol Cu^{2+}).

When the bpy-terminated SAM is exposed to a solution containing metal ions, assuming a 1:1 binding stoichiometry, the metal ions will partition between the solvated and bound state according to eq 1:

$$\text{bpy} + M \rightleftharpoons \text{bpy}{\cdot}M \tag{1}$$

Exposure to the solution of metal ions causes the system to equilibrate according to a first order rate equation:

$$d[\text{bpy}{\cdot}M]/dt = k_{on}[\text{bpy}][M] - k_{off}[\text{bpy}{\cdot}M] \tag{2}$$

where [bpy] (mol/cm^2) is the surface density of free receptors, [bpy · M] (mol/cm^2) is the surface density of complexed receptors, k_{on} (L/mol· s) is the rate constant of the forward reaction, and k_{off} (1/s) is the rate constant of the reverse reaction (dissociation of the metal ion from bpy). At equilibrium, d[bpy · M]/dt = 0, and the dissociation constant, K_d^{bpyM} [mol/L], is defined as follows:

$$K_d^{\text{bpy}{\cdot}M} \equiv \frac{k_{off}}{k_{on}} = \frac{[\text{bpy}][M]}{[\text{bpy}{\cdot}M]} \tag{3}$$

To determine the equilibrium dissociation constant from our titration experiments, we assumed that the current density through the junction (J, Amps/cm^2 of geometrical contact area) correlates linearly with the fraction of bpy groups bound to metal ions by eqs 4 and 5.

$$J = \langle J^{\text{bpy}{\cdot}M}\rangle\theta + \langle J^{\text{bpy}}\rangle(1-\theta) \tag{4}$$

$$\theta \equiv \frac{[\text{bpy}{\cdot}M]}{[\text{bpy}] + [\text{bpy}{\cdot}M]} \tag{5}$$

Here, θ is the fraction of bpy groups that are bound to metal ions, $\langle J^{\text{bpy}\cdot M}\rangle$ (amps/cm^2) is the mean current density through the EGaIn junctions in which all the bpy groups are bound to a metal ion, and $\langle J^{\text{bpy}}\rangle$ (amps/cm^2) is the mean current density through the EGaIn junctions in which none of the bpy groups are bound to metal ions. The model assumes that the area of the SAM in contact with the EGaIn tip, while not necessarily the area estimated by microscopy, is consistent from one sample to the next, and that measurements of J obtained from these areas are representative of the composition of the entire surface. We note that this model neglects the potential influence of nonlinear effects (e.g., interactions with nearest neighbor molecules that influence tunneling rates), and while this assumption was experimentally justified using XPS characterization as an independent measure of surface

https://doi.org/10.1021/jacs.1c01800
J. Am. Chem. Soc. 2021, 143, 5967–5977

composition, such effects may require consideration in other systems.

Influence of Metal Ions. We first confirmed the $J-V$ characteristics of uncomplexed junctions of the form $Au^{TS}/S(CH_2)_{11}bpy//Ga_2O_3/EGaIn$. The results are shown in Figure 2a in comparison to an alkyl thiolate SAM of similar thickness. In agreement with previous results,[32] we observed a rectification ratio of $R = 82$ with a log-standard deviation of 2.

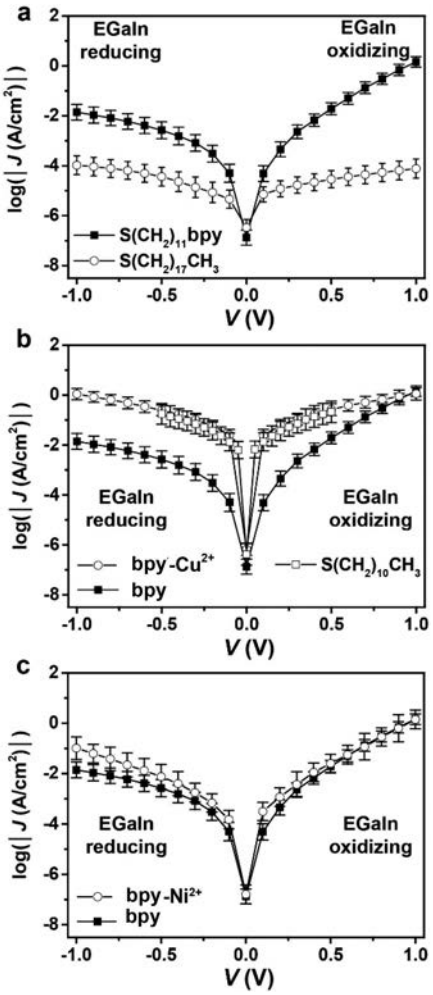

Figure 2. Charge transport through bpy–SAM junctions saturated with coordinated metal ions. (a) Control $J-V$ curves for the $Au^{TS}-S(CH_2)_{11}bpy$ junction, including a comparison to pure tunneling through $Au^{TS}-S(CH_2)_{17}CH_3$ junctions. A comparison between the $J-V$ curves for an uncomplexed junction and one saturated with (b) Cu^{2+} and (c) Ni^{2+} cations. In (b), the $J-V$ curves for $Au^{TS}-S(CH_2)_{10}CH_3$ are terminated at 0.5 V due to electrical breakdown of the junction at higher voltages. The error bars in these plots represent one log standard deviation of $\log(J)$.

Next, we established the $J-V$ characteristics of the fully complexed junctions. To do so, we prepared junctions of the form $Au^{TS}/S(CH_2)_{11}bpy(M^{n+})X_n^-//Ga_2O_3/EGaIn$, where M^{n+}, $(X^-)_n$ = Cu^{2+}, $(Cl^-)_2$ (Figure 2b), and Ni^{2+},$(Cl^-)_2$ (Figure 2c), by incubating the bpy SAMs in 1.0 mM solutions of metal salts in ethanol, rinsing with ethanol for 30 s, and drying under nitrogen gas. Figure S3 shows the junctions with M^{n+}, $(X^-)_n$ = Ag^+, (ClO_4^-), which exhibit $J-V$ characteristics similar to those of junctions with Cu^{2+}. For notational compactness we will refer to junctions of this type as bpy–M^{n+} junctions, where M^{n+} is Cu^{2+}, Ni^{2+}, or Ag^+.

Incubation of the SAMs in solutions with concentrations 1 order of magnitude higher (10 mM), followed by the same rinsing and drying procedure, resulted in the same $J-V$ characteristics, indicating that the bpy-terminated SAMs were saturated with metal ions at equilibrium for concentrations above 1 mM. The $J-V$ curves of the saturated junctions show that both Cu^{2+} and Ag^+ metal ions (see XPS spectra in Figure S5 for evidence of oxidation states of bound ions, and Figure S3 for Ag^+ data) influence the current density and rectification of the junctions, in a similar way. Introducing Cu^{2+} metal ions into the bpy junctions caused the current density to increase by almost 2 orders of magnitude ($\approx \times 75$) when the EGaIn electrode is reducing (−1.0 V). At the opposite bias, when EGaIn is oxidizing (+1.0 V), the current density remained the same ($\approx \times 1.5$), within experimental uncertainty. This difference resulted in a reduction in the rectification ratio from $R \approx 82$ in bpy junctions, to nearly to unity in bpy–Cu^{2+} junctions: $R \approx 2$, a value we regard as indicating no rectification. We attribute the elimination of rectification in bpy–Cu^{2+} junctions to a change in the energy of the HOMO with respect to the uncomplexed bpy: the shifting of the HOMO into the bias window of the junction at a negative bias causes charge transport to proceed by a hopping step to the bpy–Cu^{2+}unit, followed by a direct tunneling step across the aliphatic chain, as we have previously demonstrated.[36]

The introduction of Ni^{2+} had a smaller effect on the $J-V$ curves, relative to the effect of Cu^{2+} and Ag^+. The current density at −1.0 V increased by only 1 order of magnitude, which reduced the rectification ratio to $R = 7$ (Figure 2c). We observed that the formation of complexes with metal ions influenced the current densities of the junctions most strongly at −1.0 V and used the values of J at −1.0 V for the tunneling titrations that determined the binding kinetics for these complexes. In general, the changes in current density at negative bias may not be more prominent than the changes in current density at positive bias; the applied potential with the most prominent change in current density between the uncomplexed and complexed surface should be analyzed to minimize the influence of noise on the analysis.

Kinetics of Complex Formation and Dissociation. To establish that our rinsing procedure did not appreciably dissociate bound metal ions, we performed kinetic experiments by measuring the change in $J(-1.0\ V)$ after rinsing the saturated chip with anhydrous ethanol for varied periods of time using a syringe pump. These measurements allowed us to calculate rate constant for dissociation: k_{off} [1/s] . Figure 3a,b shows $J(-1.0\ V)$ as a function of the time that the saturated bpy–M SAMs were rinsed with anhydrous ethanol. We observed that the current densities were independent of rinsing time for rinses under 30 s, indicating that this procedure leads to no appreciable dissociation of metal ions and that the $J-V$ curves presented in Figure 2b,c represent current densities through saturated junctions, $\langle J^{bpy \cdot M} \rangle$. For these rinses, with $[M] = 0$, the rate equation can be written as follows:

$$\frac{d[\text{bpy}\cdot M]}{dt} = -k_{off}[\text{bpy}\cdot M] \quad (6)$$

Integrating this equation with respect to time, and combining the result with eq 4 results in the relation given in eq 7:

https://doi.org/10.1021/jacs.1c01800
J. Am. Chem. Soc. 2021, 143, 5967−5977

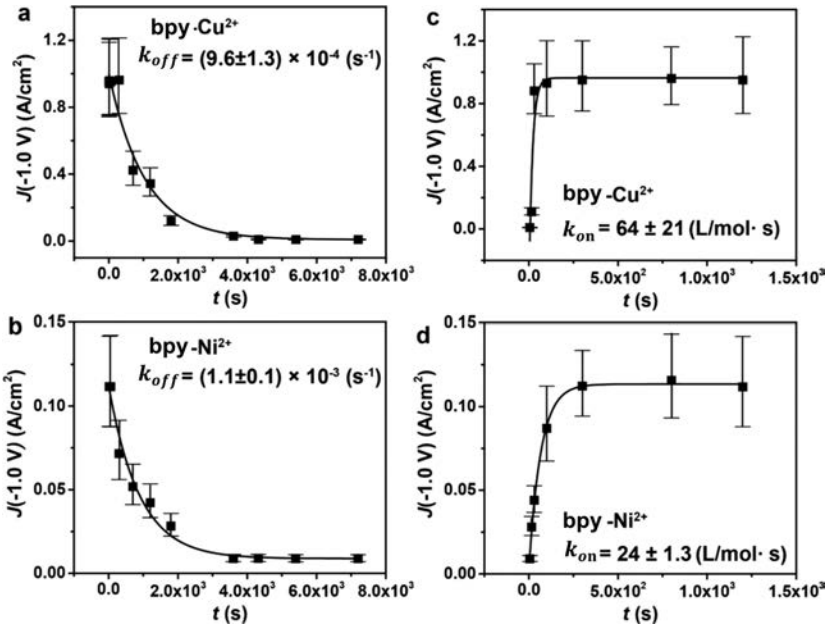

Figure 3. Kinetics of bpy−metal complex formation and dissociation. Plots showing the evolution in $J(-1.0\ \mathrm{V})$ as a function of the time that the chip was rinsed with ethanol for (a) $CuCl_2$ and (b) $NiCl_2$. Plots showing the evolution in $J(-1.0\ \mathrm{V})$ as a function of the time that the chip was incubated in a 5×10^{-4} mol/L ethanolic solution of (c) $CuCl_2$ and (d) $NiCl_2$. The solid lines represent best fits to eqs 7(a,b) and 8(c,d). Error bars denote 95% confidence interval.

$$J = (\langle J^{\mathrm{bpy}\cdot M}\rangle - \langle J^{\mathrm{bpy}}\rangle)e^{-k_{\mathrm{off}}t} + \langle J^{\mathrm{bpy}}\rangle \quad (7)$$

Taking $\langle J^{\mathrm{bpy}\cdot\mathrm{Cu}}\rangle = 0.9\ \mathrm{A/cm^2}$, $\langle J^{\mathrm{bpy}\cdot\mathrm{Ni}}\rangle = 0.1\ \mathrm{A/cm^2}$ and $\langle J^{\mathrm{bpy}}\rangle = 0.01\ \mathrm{A/cm^2}$, this exponential function can be fit to the time series in Figure 3a,b (and Figure S3) to estimate $k_{\mathrm{off}} = (9.6 \pm 1.3) \times 10^{-4}\ \mathrm{s^{-1}}$ for Cu^{2+} and $k_{\mathrm{off}} = (1.1 \pm 0.1) \times 10^{-3}\ \mathrm{s^{-1}}$ for Ni^{2+}. Thus, the difference in k_{off} between Cu^{2+} and Ni^{2+} is within experimental uncertainty. Knowledge of k_{off} enables the quantitative confirmation that the rinsing procedure results in negligible dissociation of metal ions. So long as the dimensionless parameter $\tau_{\mathrm{rinse}}k_{\mathrm{off}} \ll 1$ (where τ_{rinse} [s] is the rinsing time) rinsing does not observably affect the surface composition. For the bpy−metal complexes examined here, $\tau_{\mathrm{rinse}}k_{\mathrm{off}} \cong 0.03$ in all three cases.

We next established the association rates, k_{on} (L/mol·s), by measuring $J(-1\ \mathrm{V})$ of SAMs that were incubated for various times in solutions of metal cations ($[M] = 5 \times 10^{-4}$ mol/L) (Figure 3c,d). These experiments can be described by the full rate equation given in eq 2. This rate equation can be integrated with respect to time (assuming $[M]$ to be constant) and rearranged (see SI S5 to give the following relationship between current density and time:

$$J = (\langle J^{\mathrm{bpy}\cdot\mathrm{M}}\rangle - \langle J^{\mathrm{bpy}}\rangle)\frac{k_{\mathrm{on}}[\mathrm{M}]}{k_{\mathrm{on}}[M] + k_{\mathrm{off}}}(1 - e^{-k_{\mathrm{on}}[\mathrm{M}]t - k_{\mathrm{off}}t}) + \langle J^{\mathrm{bpy}}\rangle \quad (8)$$

Using the values obtained from these experiments, we can estimate the value of K_{d} by $K_{\mathrm{d}} = k_{\mathrm{off}}/k_{\mathrm{on}}$. For bpy−$Cu^{2+}$, $K_{\mathrm{d}} = 1.5 \times 10^{-5}$ mol/L, and for bpy−Ni^{2+}, $K_{\mathrm{d}} = 4.5 \times 10^{-5}$ mol/L. These values of K_{d} are comparable with the values obtained by the titration method (see below).

Titration to Obtain Dissociation Constant (K_{d}). To measure the dissociation constants of the metal−bpy complexes we also performed titration experiments. Our titration experiments can be described mathematically by combining eqs 3 and 4 with a conservation argument for the bpy groups. Following algebraic manipulation (SI S5) the current density can be related to the dissociation constant and the concentration of metal ions in solution by the following equation:

$$\log\left(\frac{J - \langle J^{\mathrm{bpy}\cdot M}\rangle}{\langle J^{\mathrm{bpy}}\rangle - J}\right) = \log(K_{\mathrm{d}}^{\mathrm{bpy}\cdot M}) - \log([M]) \quad (9)$$

This equation implies that, if this simple equilibrium binding model (assuming a 1:1 stoichiometry of binding) is appropriate, then a plot of $\log\left(\frac{J - \langle J^{\mathrm{bpy}\cdot M}\rangle}{\langle J^{\mathrm{bpy}}\rangle - J}\right)$ vs $\log([M])$ will be linear with a slope equal to −1 and a y-intercept equal to $\log(K_{\mathrm{d}}^{\mathrm{bpy}\cdot M})$.

Figure 4a−d shows the results of our titration experiments with Cu^{2+}. $J(-1.0\ \mathrm{V})$ changes from ∼0.9 $\mathrm{Acm^{-2}}$ at $[Cu^{2+}] = 10^{-7}$ M to $J \approx 0.01\ \mathrm{Acm^{-2}}$ at $[Cu^{2+}] = 10^{-4}$ mol/L (Figure 4b). The method of least-squares was used to fit eq 9 to the data (Figure 4c), yielding a dissociation constant of $K_{\mathrm{d}}^{Cu^{2+}} = 1.9 \times 10^{-5}$ mol/L. The fit in Figure 4c indicates that the simple binding model holds for this system, with a plot of $\log\left(\frac{J - \langle J^{\mathrm{bpy}\cdot M}\rangle}{\langle J^{\mathrm{bpy}}\rangle - J}\right)$ vs $\log([M])$ giving a line of slope −1 and a y-intercept of $\log(K_{\mathrm{d}})$. Figure 4e−h shows the results of our titration experiments with Ni^{2+}. The dissociation constant inferred from these experiments was $K_{\mathrm{d}}^{Ni^{2+}} = 1.3 \times 10^{-4}$ mol/L. Comparing to the values of the dissociation constant measured in solution (Table 1), these values follow the same qualitative trend (i.e., $K_{\mathrm{d}}^{Ni^{2+}}$ is about 1 order of magnitude higher than $K_{\mathrm{d}}^{Cu^{2+}}$), however, they are both several orders of magnitude larger than the value in solution. We believe that this reduction in the stability of the surface-bound chelate in comparison to the solution-phase could arise in part due to entropic effects (i.e., the surface-bound chelate has a larger reduction in entropy upon binding than the solution-phase chelate).

https://doi.org/10.1021/jacs.1c01800
J. Am. Chem. Soc. 2021, 143, 5967−5977

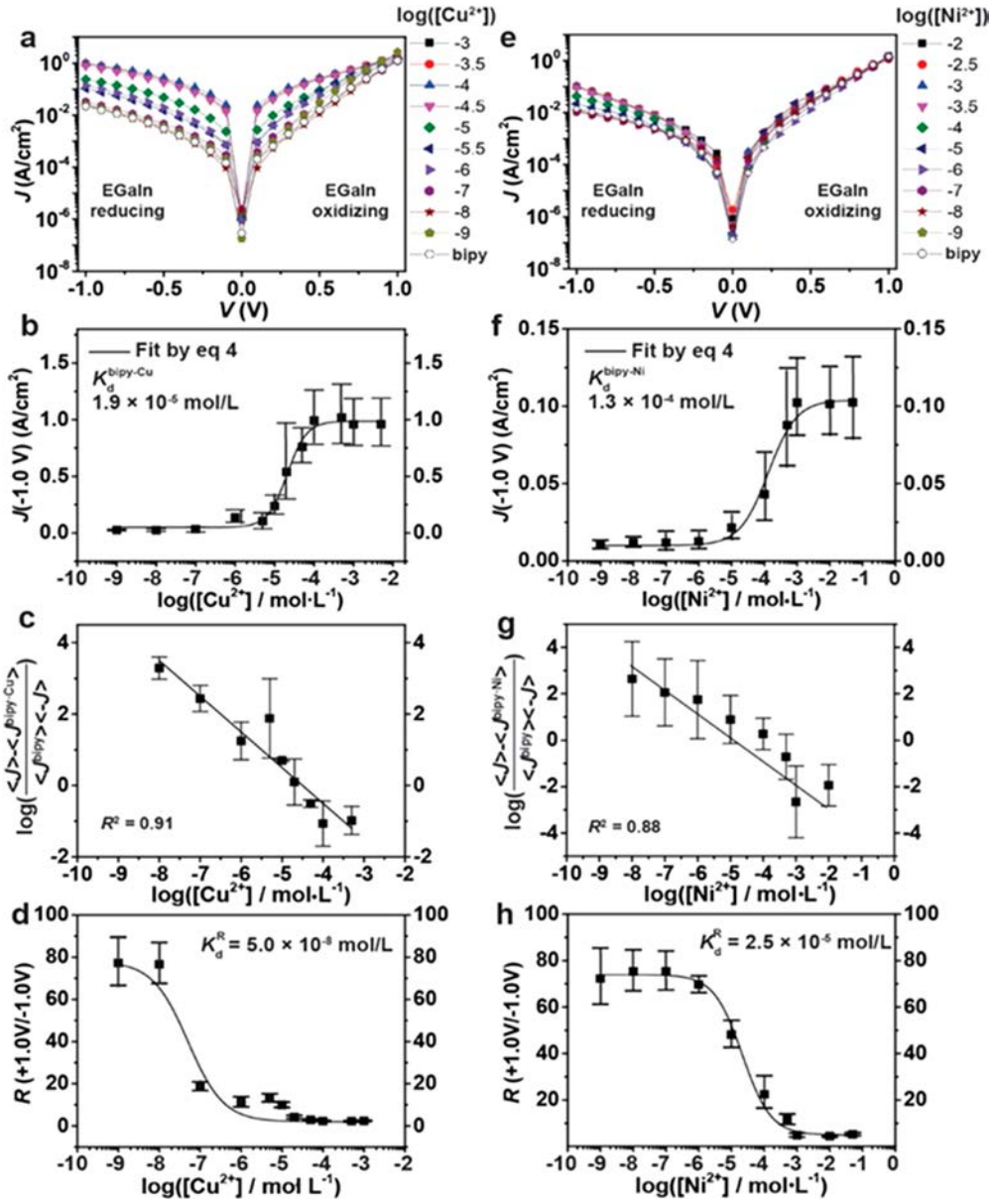

Figure 4. Results of tunneling titration experiments. Evolution of $J-V$ curves after incubation in ethanolic solutions of varied concentration of (a) Cu^{2+} and (e) Ni^{2+} cations. Error bars are omitted for clarity. Titration curve showing the sigmoidal shape of $|J(-1.0\ V)|$ as a function of concentration of (b) Cu^{2+} and (f) Ni^{2+} cations. Error bars for J represent 95% confidence intervals of the mean value. Plot showing a linear regression fit to eq 9 for the (c) Cu^{2+} and (g) Ni^{2+} titration with error bars representing 95% confidence intervals, obtained by the propagating the uncertainty in the measured current densities through the formula on the y-axis. Plots showing the evolution of the rectification ratio as a function of (d) Cu^{2+} and (h) Ni^{2+} cation concentrations in solution. Error bars for R represent one log-standard deviation.

The rectification ratio, $R = |J(+1.0\ V)|/|J(-1.0\ V)|$, provides another potential method of estimating K_d. Since, $J(+1.0\ V)$ is essentially unchanged by the binding of the metal, while this increases $J(-1.0\ V)$, a plot of R vs $\log[Cu^{2+}]$ (Figure 4g) also has a sigmoidal shape with its inflection point yielding $K_d^R = 5.0 \times 10^{-8}$ mol/L for Cu^{2+} and 2.5×10^{-4} mol/L for Ni^{2+}. For the Cu^{2+} titration, there is one data point at a concentration of 10^{-7} mol/L that has an anomalously low rectification ratio, which we determined to be the result of an decrease in $J(+1.0\ V)$ rather than an increase of $J(-1.0\ V)$. It is unclear what the cause of this observation is, as XPS measurements of this sample did not reveal the presence of any Cu^{2+} ions.

Competitive Titration. To build upon the titration experiments with a single metal ion, it is also of interest to measure the competitive binding of two metal ions with SAMs terminated in bpy groups. Here, we introduce the equations to describe the tunneling titration experiments of two metal ions ($M1$ and $M2$), both present in solution, and competing for bpy groups, again assuming a 1:1 binding stoichiometry between each metal ion and bpy. The equilibrium equations are as follows:

$$\text{bpy} + M1 \rightleftharpoons \text{bpy}{\cdot}M1 \tag{10}$$

$$\text{bpy} + M2 \rightleftharpoons \text{bpy}{\cdot}M2 \tag{11}$$

$$K_d^{\text{bpy}\cdot M1} = \frac{[\text{bpy}][M1]}{[\text{bpy}{\cdot}M1]} \tag{12}$$

https://doi.org/10.1021/jacs.1c01800
J. Am. Chem. Soc. 2021, 143, 5967−5977

$$K_d^{bpy\cdot M2} = \frac{[bpy][M2]}{[bpy\cdot M2]} \tag{13}$$

Following a line of reasoning analogous to that used with the binding model for the single metal ion (see SI S5), the total current density through a junction containing a bpy-terminated SAM that has been incubated in a solution containing two metal ions can be written as follows:

$$J = \frac{\langle J^{bpy\cdot M1}\rangle [M1]}{\left(K_d^{bpy\cdot M1} + [M1] + [M2]\frac{K_d^{bpy\cdot M1}}{K_d^{bpy\cdot M2}}\right)} + \frac{\langle J^{bpy\cdot M2}\rangle [M2]}{\left(K_d^{bpy\cdot M2} + [M2] + [M1]\frac{K_d^{bpy\cdot M2}}{K_d^{bpy\cdot M1}}\right)} + \frac{\langle J^{bpy}\rangle}{\left(1 + \frac{[M1]}{K_d^{bpy\cdot M1}} + \frac{[M2]}{K_d^{bpy\cdot M2}}\right)} \tag{14}$$

A more detailed description of this derivation and analysis of the limits of eq 14 can be found in SI S5.

Since junctions containing Cu^{2+} and Ni^{2+} have values of $J(-1.0\ V)$ that differ by 1 order of magnitude, we chose these two metal ions to perform competitive binding experiments. For these experiments the total concentration of metal ions was held constant at 1 mM, and the molar ratio of Cu^{2+}: Ni^{2+} was systematically varied. Using the values of the dissociation constant and current densities obtained from the single-component titration experiments, along with eq 14, allowed a quantitative prediction for the expected results to be made. Figure 5 shows a comparison between the expected trend from eq 14 with $K_d^{Cu^{2+}} = 1.9 \times 10^{-5}$ mol/L and $K_d^{Ni^{2+}} = 1.3 \times 10^{-4}$ mol/L (solid line), and the experimental results. This agreement serves to validate the values of the dissociation constant, and competitive binding constants.

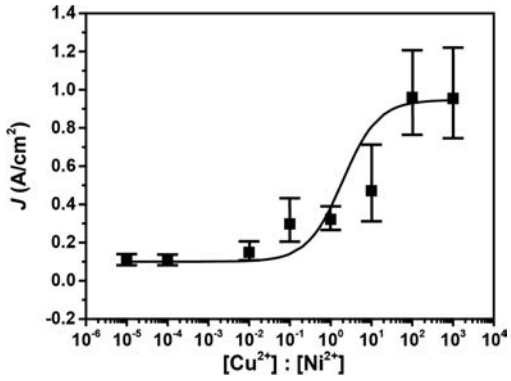

Figure 5. Competitive binding curve for Cu^{2+} and Ni^{2+}, showing the current density obtained after incubating $Au^{TS}/S(CH_2)_{11}bpy$ in ethanol solutions containing $CuCl_2$ and $NiCl_2$ of varied molar ratio for 12 h under ambient conditions (with a constant total concentration 10^{-3} mol/L). The solid black line represents a prediction made using eq 14 with $K_d^{Cu^{2+}} = 1.9 \times 10^{-5}$ mol/L and $K_d^{Ni^{2+}} = 1.3 \times 10^{-4}$ mol/L, obtained from the single metal ion titration experiments. Error bars represent 95% confidence intervals of the current density.

XPS Characterization. The Cu 2*p*, Ni 2*p*, and Ag 3*d* spectra (Figure S2) confirmed the oxidation states of Cu^{2+}, Ni^{2+}, and Ag^+ in the complexes with bpy-terminated SAMs. As described in detail in SI S4, care was required in interpreting the XPS data from bpy−Cu^{2+} complexes, we found that a small fraction of the Cu^{2+} were reduced to Cu^+ by photoelectrons. We calculated the ratios of cations to anions from the intensities of the respective peaks in the XPS spectra, finding 1:2 ratios of Cu^{2+} and Ni^{2+} to chloride anions, and a 1:1 ratio of Ag^+ to perchlorate anions (see details in SI S4).

Coordination Structure. In solution, 1:1 bpy/M complexes have distorted tetrahedral geometries[44,45] for M^{n+} = Cu^{2+} and $Ni^{2+}$and a distorted T-shaped geometry[46] for M^{n+} = Ag^+. We do not observe any differences in the binding energies of the metal ions for samples prepared with different $[M]$, as might be expected were the number of ligands per metal different at lower than at higher concentrations. The ratios of nitrogen to metal atoms are also consistent with a 1:1 coordination of bpy−M^{n+} complex at high [M] (=10^{-2} to 10^{-4} mol/L for $[Cu^{2+}]$ and $[Ag^+]$, and 10^{-1} to 10^{-3} mol/L for $[Ni^{2+}]$ (Figure 6).

To verify the results obtained from the tunneling titration experiments, we performed an analogous experimental procedure and analysis using the elemental ratio (ER) of metal ion to nitrogen atom from XPS as the titration observable. As shown in Figure 6, we observed a similar sigmoidal curve, that could be fit to a standard Langmuir adsorption model:

$$ER = \frac{1}{2}\frac{[M]}{K_d + [M]} \tag{15}$$

where ER denotes elemental ratio of metal ion to nitrogen. A fit of the data to eq 15 yields values of $K_d^{Cu} = 4.7 \times 10^{-6}$ mol/L $K_d^{Ni} = 9.4 \times 10^{-5}$ mol/L and $K_d^{Ag} = 3.3 \times 10^{-6}$ mol/L. In all cases the XPS titration yields values that are in good qualitative agreement with those obtained through tunneling titration (see Table 1).

CONCLUSIONS

This work describes a technique that allows the EGaIn junction to be used to characterize tunneling through monolayers whose components are reversibly bound. Through measurements of tunneling currents and the development of a mathematical model, we demonstrate how best the EGaIn junction can be used to examine noncovalent binding of ligands on a surface using tunneling current density as an observable. All previous work with the EGaIn junction employed monolayers of fixed composition to understand how molecular structure influences charge tunneling. We demonstrate here that the EGaIn junction can be used to perform surface-sensitive titrations and kinetics experiments to infer the dissociation constants and kinetic rate constants of noncovalent complexes (in this case, ligand−metal binding) formed on the surface of a SAM.

We determined an appropriate procedure for sample preparation—including control of complexation time, rinsing, and drying of samples—to ensure that the bpy−M complexes on the surface represent an equilibrium state during the tunneling measurements, which are performed ex situ. A simple 1:1 binding stoichiometry was observed for all three metals. An equilibrium binding model was derived and used to infer the binding constants of Cu^{2+}, Ag^+, and Ni^{2+} to bpy from $J(-1.0\ V)$, yielding results comparable to those obtained by XPS. We found that complexation of bpy-terminated SAMs with these metal ions generally increased the tunneling current at a given voltage with respect to the uncomplexed SAMs. The increases of $J(-1.0\ V)$ were much greater than those of $J(+1.0\ V)$, and for Cu^{2+} and Ag^+, these changes in $J(-1.0\ V)$ were

https://doi.org/10.1021/jacs.1c01800
J. Am. Chem. Soc. 2021, 143, 5967−5977

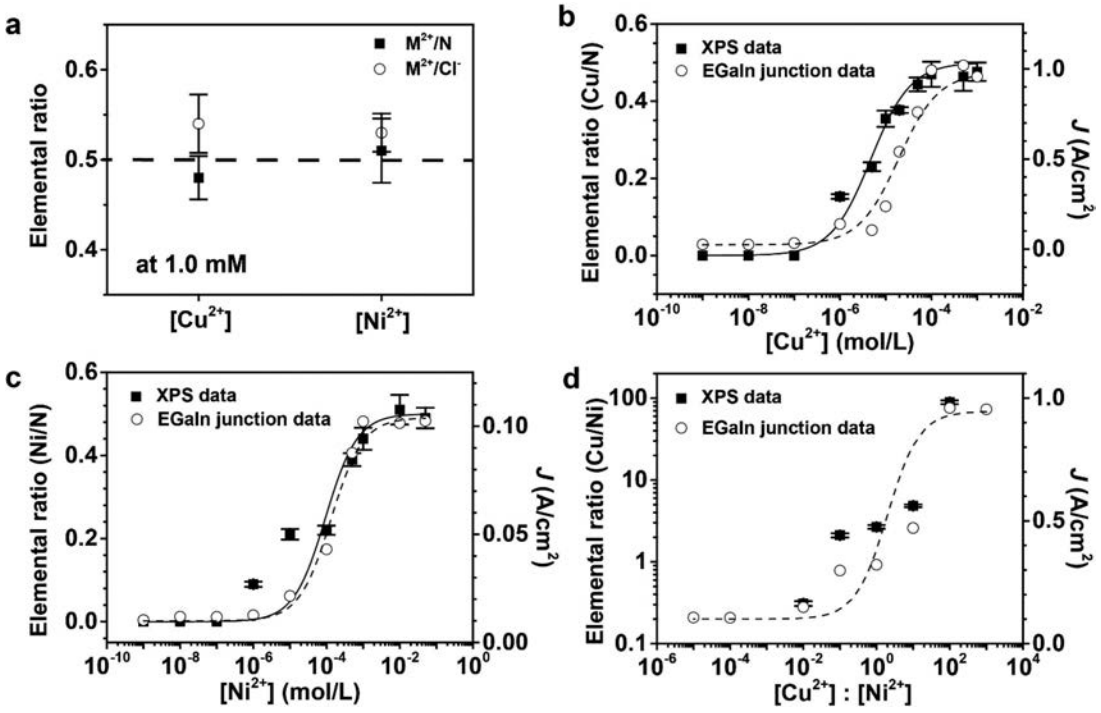

Figure 6. Comparison of data from XPS and tunneling titrations. (a) The elemental ratio obtained from XPS data for a fully complexed surface. Plots showing the elemental ratio of (b) Cu^2 and (c) Ni^{2+} to nitrogen obtained from XPS, together with currents measured with the EGaIn junction on monolayers prepared in the same way. The solid lines are the fits to XPS data using eq 15 and the dashed lines are the fits to tunneling data using eq 9. (d) Plot showing the ratio of bound Cu^{2+} to Ni^{2+} ions from the competitive binding experiments obtained from XPS in comparison the currents measured with the EGaIn junction. Error bars in the data from EGaIn junctions are omitted for clarity. Error bars in the XPS data represent the peak fitting error.

sufficient to effectively eliminate the rectification observed with the bpy-terminated SAM. We found that the values for K_d on the surface were substantially different from those reported by others in solution. We attribute these discrepancies to differences in preferred binding stoichiometry, constraints associated with the tethered bpy group (i.e., a larger reduction in entropy of the association reaction), and differences in solvation between surface-bound complexes and complexes in solution.

The simple and accessible method introduced here provides information complementary to that obtained by conventional instrumental approaches, such as XPS. The advantages of this technique are that it is sensitive, nondestructive, and employs a relatively simple and inexpensive experimental set up that does not require vacuum conditions, X-rays, or laser technology.

The disadvantages are the levels of noise in the measured currents and the time required to generate adequate statistics. The tunneling titration would be the best approach to characterizing the binding kinetics for a system in which the bound complex would dissociate in a vacuum environment, such as the 10^{-7} mbar pressure required for the XPS measurements in this paper. This method would also be ideal for samples too delicate for, or of elemental compositions that are inconvenient for, XPS analysis.

While this study focused specifically on metal ions bound to bpy-terminated SAMs, this titration technique should be capable of studying noncovalently bound organic adsorbents deposited on a substrate either from the solution, or from the vapor phase. Moreover, this work demonstrates the EGaIn junction as an analytical technique to infer details about the composition of a surface, and thus represents a new research direction and an initial step toward bridging molecular electronics with surface-based supramolecular chemistry.

■ ASSOCIATED CONTENT

Supporting Information

The Supporting Information is available free of charge at https://pubs.acs.org/doi/10.1021/jacs.1c01800.

S1, materials; S2, histograms of tunneling currents from the titration of Cu^{2+}; S3, bpy–Ag titration; S4, X-ray photoelectron spectroscopy; and S5, binding model (PDF)

■ AUTHOR INFORMATION

Corresponding Author

George M. Whitesides − *Department of Chemistry and Chemical Biology, Harvard University, Cambridge, Massachusetts 02138, United States;* orcid.org/0000-0001-9451-2442; Email: gwhitesides@gmwgroup.harvard.edu

Authors

Yuan Li − *Department of Chemistry and Chemical Biology, Harvard University, Cambridge, Massachusetts 02138, United States; Department of Chemistry, Tsinghua University, Beijing 100084, P. R. China*

Samuel E. Root − *Department of Chemistry and Chemical Biology, Harvard University, Cambridge, Massachusetts 02138, United States*

Lee Belding − *Department of Chemistry and Chemical Biology, Harvard University, Cambridge, Massachusetts 02138, United States*

https://doi.org/10.1021/jacs.1c01800
J. Am. Chem. Soc. 2021, 143, 5967−5977

Junwoo Park − *Department of Chemistry and Chemical Biology, Harvard University, Cambridge, Massachusetts 02138, United States*

Jeff Rawson − *Department of Chemistry and Chemical Biology, Harvard University, Cambridge, Massachusetts 02138, United States;* orcid.org/0000-0002-8431-0772

Hyo Jae Yoon − *Department of Chemistry, Korea University, Seoul 02841, Korea;* orcid.org/0000-0002-2501-0251

Mostafa Baghbanzadeh − *Department of Chemistry and Chemical Biology, Harvard University, Cambridge, Massachusetts 02138, United States;* orcid.org/0000-0001-7678-1681

Philipp Rothemund − *Department of Chemistry and Chemical Biology and John A. Paulson School of Engineering and Applied Sciences, Harvard University, Cambridge, Massachusetts 02138, United States*

Complete contact information is available at: https://pubs.acs.org/10.1021/jacs.1c01800

Author Contributions

[⊥]These authors contributed equally to this work.

Notes

The authors declare no competing financial interest.

■ ACKNOWLEDGMENTS

This work was supported by the National Science Foundation (NSF, CHE-1808361). We acknowledge the Materials Research and Engineering Center (MRSEC, DMR-1420570) at Harvard University for supporting XPS measurements and providing access to the clean room facilities. Sample preparation and characterization was performed in part at the Center for Nanoscale Systems (CNS) at Harvard University, a member of the National Nanotechnology Infrastructure Network (NNIN), which is supported by the National Science Foundation (ECS0335765). L.B. acknowledges salary support from the Simons Foundation (award 290364FY18). J.P. acknowledges fellowship support from the Basic Science Research Program through the National Research Foundation of Korea (NRF), funded by the Ministry of Education of Korea (2018R1A6A3A03013079). H.J.Y. acknowledges the support from the NRF of Korea (NRF-2019R1A2C2011003 and NRF-2019R1A6A1A11044070). We thank Darrell Collison, Brian Cafferty, and Victoria E. Campbell for their discussions and preliminary experiments.

■ REFERENCES

(1) Ashcroft, N. W.; Mermin, N. D. *Solid State Physics*, 1st ed.; Saunders College Publishing: New York, 1976.

(2) Xiang, D.; Wang, X.; Jia, C.; Lee, T.; Guo, X. Molecular-Scale Electronics: From Concept to Function. *Chem. Rev.* **2016**, *116* (7), 4318−4440.

(3) Haick, H.; Cahen, D. Contacting Organic Molecules by Soft Methods: Towards Molecule-Based Electronic Devices. *Acc. Chem. Res.* **2008**, *41* (3), 359−366.

(4) Mrksich, M.; Sigal, G. B.; Whitesides, G. M. Surface Plasmon Resonance Permits in Situ Measurement of Protein Adsorption on Self-Assembled Monolayers of Alkanethiolates on Gold. *Langmuir* **1995**, *11* (11), 4383−4385.

(5) Marx, K. A. Quartz Crystal Microbalance: A Useful Tool for Studying Thin Polymer Films and Complex Biomolecular Systems at the Solution - Surface Interface. *Biomacromolecules* **2003**, *4* (5), 1099−1120.

(6) Stora, T.; Hovius, R.; Dienes, Z.; Pachoud, M.; Vogel, H. Metal Ion Trace Detection by a Chelator-Modified Gold Electrode: A Comparison of Surface to Bulk Affinity. *Langmuir* **1997**, *13* (20), 5211−5214.

(7) Mandler, D.; Kraus-Ophir, S. Self-Assembled Monolayers (SAMs) for Electrochemical Sensing. *J. Solid State Electrochem.* **2011**, *15* (7−8), 1535−1558.

(8) Xiao, X.; Xu, B.; Tao, N. Conductance Titration of Single-Peptide Molecules. *J. Am. Chem. Soc.* **2004**, *126* (17), 5370−5371.

(9) Cademartiri, L.; Thuo, M. M.; Nijhuis, C. A.; Reus, W. F.; Tricard, S.; Barber, J. R.; Sodhi, R. N. S.; Brodersen, P.; Kim, C.; Chiechi, R. C.; Whitesides, G. M. Electrical Resistance of Ag TS-S(CH 2) n −1CH 3//Ga 2O 3/EGaIn Tunneling Junctions. *J. Phys. Chem. C* **2012**, *116* (20), 10848−10860.

(10) Simeone, F. C.; Yoon, H. J.; Thuo, M. M.; Barber, J. R.; Smith, B.; Whitesides, G. M. Defining the Value of Injection Current and Effective Electrical Contact Area for Egain-Based Molecular Tunneling Junctions. *J. Am. Chem. Soc.* **2013**, *135* (48), 18131−18144.

(11) Bowers, C. M.; Rappoport, D.; Baghbanzadeh, M.; Simeone, F. C.; Liao, K. C.; Semenov, S. N.; Zaba, T.; Cyganik, P.; Aspuru-Guzik, A.; Whitesides, G. M. Tunneling across SAMs Containing Oligophenyl Groups. *J. Phys. Chem. C* **2016**, *120* (21), 11331−11337.

(12) Liao, K. C.; Yoon, H. J.; Bowers, C. M.; Simeone, F. C.; Whitesides, G. M. Replacing AgTSSCH2-R with AgTSO 2C-R in EGaIn-Based Tunneling Junctions Does Not Significantly Change Rates of Charge Transport. *Angew. Chem., Int. Ed.* **2014**, *53* (15), 3889−3893.

(13) Baghbanzadeh, M.; Simeone, F. C.; Bowers, C. M.; Liao, K. C.; Thuo, M.; Baghbanzadeh, M.; Miller, M. S.; Carmichael, T. B.; Whitesides, G. M. Odd-Even Effects in Charge Transport across n-Alkanethiolate-Based SAMs. *J. Am. Chem. Soc.* **2014**, *136* (48), 16919−16925.

(14) Belding, L.; Root, S. E.; Li, Y.; Park, J.; Baghbanzadeh, M.; Rojas, E.; Pieters, P. F.; Yoon, H. J.; Whitesides, G. M. Conformation, and Charge Tunneling through Molecules in SAMs. *J. Am. Chem. Soc.* **2021**, *143*, 3481−3493.

(15) Wimbush, K. S.; Fratila, R. M.; Wang, D.; Qi, D.; Liang, C.; Yuan, L.; Yakovlev, N.; Loh, K. P.; Reinhoudt, D. N.; Velders, A. H.; Nijhuis, C. A. Bias Induced Transition from an Ohmic to a Non-Ohmic Interface in Supramolecular Tunneling Junctions with Ga2O3/EGaIn Top Electrodes. *Nanoscale* **2014**, *6* (19), 11246−11258.

(16) Nerngchamnong, N.; Yuan, L.; Qi, D. C.; Li, J.; Thompson, D.; Nijhuis, C. A. The Role of van Der Waals Forces in the Performance of Molecular Diodes. *Nat. Nanotechnol.* **2013**, *8* (2), 113−118.

(17) Yuan, L.; Nerngchamnong, N.; Cao, L.; Hamoudi, H.; Del Barco, E.; Roemer, M.; Sriramula, R. K.; Thompson, D.; Nijhuis, C. A. Controlling the Direction of Rectification in a Molecular Diode. *Nat. Commun.* **2015**, *6* (1), 1−11.

(18) Carlotti, M.; Degen, M.; Zhang, Y.; Chiechi, R. C. Pronounced Environmental Effects on Injection Currents in EGaIn Tunneling Junctions Comprising Self-Assembled Monolayers. *J. Phys. Chem. C* **2016**, *120* (36), 20437−20445.

(19) Fracasso, D.; Valkenier, H.; Hummelen, J. C.; Solomon, G. C.; Chiechi, R. C. Evidence for Quantum Interference in Sams of Arylethynylene Thiolates in Tunneling Junctions with Eutectic Ga-In (EGaIn) Top-Contacts. *J. Am. Chem. Soc.* **2011**, *133* (24), 9556−9563.

(20) Kong, G. D.; Kim, M.; Cho, S. J.; Yoon, H. J. Gradients of Rectification: Tuning Molecular Electronic Devices by the Controlled Use of Different-Sized Diluents in Heterogeneous Self-Assembled Monolayers. *Angew. Chem., Int. Ed.* **2016**, *55* (35), 10307−10311.

(21) Kong, G. D.; Jin, J.; Thuo, M. M.; Song, H.; Joung, J. F.; Park, S.; Yoon, H. J. Elucidating the Role of Molecule−Electrode Interfacial Defects in Charge Tunneling Characteristics of Large-Area Junctions. *J. Am. Chem. Soc.* **2018**, *140*, 12303−12307.

(22) Jin, J.; Kong, G. D.; Yoon, H. J. Deconvolution of Tunneling Current in Large-Area Junctions Formed with Mixed Self-Assembled Monolayers. *J. Phys. Chem. Lett.* **2018**, *9* (16), 4578−4583.

(23) Kang, S.; Park, S.; Kang, H.; Cho, S. J.; Song, H.; Yoon, H. J. Tunneling and Thermoelectric Characteristics of N-Heterocyclic Carbene-Based Large-Area Molecular Junctions. *Chem. Commun.* **2019**, *55* (60), 8780−8783.
(24) Bruce, R. C.; You, L.; Förster, A.; Pookpanratana, S.; Pomerenk, O.; Lee, H. J.; Marquez, M. D.; Ghanbaripour, R.; Zenasni, O.; Lee, T. R.; Hacker, C. A. Contrasting Transport and Electrostatic Properties of Selectively Fluorinated Alkanethiol Monolayers with Embedded Dipoles. *J. Phys. Chem. C* **2018**, *122* (9), 4881−4890.
(25) Lenfant, S.; Viero, Y.; Krzeminski, C.; Vuillaume, D.; Demeter, D.; Dobra, I.; Oçafrain, M.; Blanchard, P.; Roncali, J.; Van Dyck, C.; Cornil, J. New Photomechanical Molecular Switch Based on a Linear π-Conjugated System. *J. Phys. Chem. C* **2017**, *121* (22), 12416−12425.
(26) Whitesides, G. M. Physical-Organic Chemistry: A Swiss Army Knife. *Isr. J. Chem.* **2016**, *56* (1), 66−82.
(27) Wimbush, K. S.; Reus, W. F.; Van Der Wiel, W. G.; Reinhoudt, D. N.; Whitesides, G. M.; Nijhuis, C. A.; Velders, A. H. Control over Rectification in Supramolecular Tunneling Junctions. *Angew. Chem., Int. Ed.* **2010**, *49* (52), 10176−10180.
(28) Tran, T. K.; Smaali, K.; Hardouin, M.; Bricaud, Q.; Oçafrain, M.; Blanchard, P.; Lenfant, S.; Godey, S.; Roncali, J.; Vuillaume, D. A Crown-Ether Loop-Derivatized Oligothiophene Doubly Attached on Gold Surface as Cation-Binding Switchable Molecular Junction. *Adv. Mater.* **2013**, *25* (3), 427−431.
(29) Bruce, R. C.; Wang, R.; Rawson, J.; Therien, M. J.; You, W. Valence Band Dependent Charge Transport in Bulk Molecular Electronic Devices Incorporating Highly Conjugated Multi-[(Porphinato)Metal] Oligomers. *J. Am. Chem. Soc.* **2016**, *138* (7), 2078−2081.
(30) Tuccitto, N.; Ferri, V.; Cavazzini, M.; Quici, S.; Zhavnerko, G.; Licciardello, A.; Rampi, M. A. Highly Conductive ∼ 40-Nm-Long Molecular Wires Assembled by Stepwise Incorporation of Metal Centres. *Nat. Mater.* **2009**, *8* (1), 41−46.
(31) Kaes, C.; Katz, A.; Hosseini, M. W. Bipyridine: The Most Widely Used Ligand. A Review of Molecules Comprising at Least Two 2,2′-Bipyridine Units. *Chem. Rev.* **2000**, *100* (10), 3553−3590.
(32) Yoon, H. J.; Liao, K. C.; Lockett, M. R.; Kwok, S. W.; Baghbanzadeh, M.; Whitesides, G. M. Rectification in Tunneling Junctions: 2,2'-Bipyridyl-Terminated n -Alkanethiolates. *J. Am. Chem. Soc.* **2014**, *136* (49), 17155−17162.
(33) Irving, H.; Mellor, D. H. The Stability of Metal Complexes of 11,10-Phenanthroline and Its Analogues. Part I. 1,10-Penanthroline and 2,2'-Bipyridyl. *J. Chem. Soc.* **1962**, *0*, 5222−5237.
(34) Irving, H.; Williams, R. J. P. Order of Stability of Metal Complexes. *Nature* **1948**, *162* (4123), 746−747.
(35) Nijhuis, C. A.; Reus, W. F.; Whitesides, G. M. Mechanism of Rectification in Tunneling Junctions Based on Molecules with Asymmetric Potential Drops. *J. Am. Chem. Soc.* **2010**, *132* (51), 18386−18401.
(36) Park, J.; Belding, L.; Yuan, L.; Mousavi, M. P. S.; Root, S. E.; Yoon, H. J.; Whitesides, G. M. Rectification in Molecular Tunneling Junctions Based on Alkanethiolates with Bipyridine − Metal Complexes. *J. Am. Chem. Soc.* **2021**, *143* (4), 2156−2163.
(37) Cabani, S.; Moretti, G.; Scrocco, E. Stability Constants of Copper(II)-2,2'-Bipyridyl Complexes. *J. Chem. Soc.* **1962**, *0*, 88−93.
(38) Kang, H.; Kong, G. D.; Byeon, S. E.; Yang, S.; Kim, J. W.; Yoon, H. J. Interplay of Fermi Level Pinning, Marcus Inverted Transport, and Orbital Gating in Molecular Tunneling Junctions. *J. Phys. Chem. Lett.* **2020**, *11* (20), 8597−8603.
(39) Kang, H.; Kong, G. D.; Yoon, H. J. Solid State Dilution Controls Marcus Inverted Transport in Rectifying Molecular Junctions. *J. Phys. Chem. Lett.* **2021**, *12* (3), 982−988.
(40) Rothemund, P.; Morris Bowers, C.; Suo, Z.; Whitesides, G. M. Influence of the Contact Area on the Current Density across Molecular Tunneling Junctions Measured with EGaIn Top-Electrodes. *Chem. Mater.* **2018**, *30* (1), 129−137.
(41) Reus, W. F.; Nijhuis, C. A.; Barber, J. R.; Thuo, M. M.; Tricard, S.; Whitesides, G. M. Statistical Tools for Analyzing Measurements of Charge Transport. *J. Phys. Chem. C* **2012**, *116* (11), 6714−6733.
(42) Watcharinyanon, S.; Puglia, C.; Göthelid, E.; Bäckvall, J. E.; Moons, E.; Johansson, L. S. O. Molecular Orientation of Thiol-Derivatized Tetraphenylporphyrin on Gold Studied by XPS and NEXAFS. *Surf. Sci.* **2009**, *603* (7), 1026−1033.
(43) Adamson, A. W.; Gast, A. P. Adsorption of Gases and Vapors on Solids *Physical Chemistry of Surfaces*, 6th ed.; John Wiley & Sons: New York, 1960, pp 599−615.
(44) Awad, D. J.; Schilde, U.; Strauch, P. 4,4′-Bis(Tert-Butyl)-2,2′-Bipyridinedichlorometal(II) -Synthesis, Structure and EPR Spectroscopy. *Inorg. Chim. Acta* **2011**, *365* (1), 127−132.
(45) Palmer, R. A.; Piper, T. S. 2,2′-Bipyridine Complexes. I. Polarized Crystal Spectra of Tris(2,2′-Bipyridine)Copper(II), -Nickel-(II), -Cobalt(II), -Iron(II), and -Ruthenium(II). *Inorg. Chem.* **1966**, *5* (5), 864−878.
(46) Bellusci, A.; Crispini, A.; Pucci, D.; Szerb, E.; Ghedini, M. Structural Variations in Bipyridine Silver(i) Complexes: Role of the Substituents and Counterions. *Cryst. Growth Des.* **2008**, *8* (8), 3114−3122.

https://doi.org/10.1021/jacs.1c01800
J. Am. Chem. Soc. 2021, 143, 5967−5977